Molecular Ecology (2008) doi: 10.1111/j.1365-294X.2007.03630.x

Determining the origin and age of the Westland beech (*Nothofagus*) gap, New Zealand, using fungus beetle genetics

RICHARD A. B. LESCHEN,* THOMAS R. BUCKLEY,* HELEN M. HARMAN* and JAMES SHULMEISTER†
*Landcare Research, Private Bag 92170, Auckland, New Zealand, †Department of Geological Sciences, University of Canterbury, Private Bag 4800, Christchurch, New Zealand

Abstract

The formation and maintenance of the *Nothofagus* beech gap in the South Island, New Zealand, has been the focus of biogeographical debate since the 1920s. We examine the historical process of gap formation by investigating the population genetics of fungus beetles: *Brachynopus scutellaris* (Staphylinidae) inhabits logs and is absent from the beech gap, and *Hisparonia hystrix* (Nitidulidae) is contiguous through the gap and is found commonly on sooty mould growing on several plant species. Both species show distinctive northern and southern haplotype distributions while *H. hystrix* recolonized the gap as shown by definitive mixing. *B. scutellaris* shows two major haplotype clades with strong geographical concordance, and unlike *H. hystrix*, has clearly defined lineages that can be partitioned for molecular dating. Based on coalescence dating methods, disjunct lineages of *B. scutellaris* indicate that the gap was formed less than 200 000 years ago. Phylogenetic imprints from both species reveal similar patterns of population divergence corresponding to recent glacial cycles, favouring a glacial explanation for the origin of the gap. Post-gap colonization by *H. hystrix* may have been facilitated by the spread of *Leptospermum scoparium* host trees to the area, and they may be better at dispersing than *B. scutellaris* which may be constrained by fungal host and/or microhabitat. The gap-excluded species *B. scutellaris* is found in both beech and podocarp-broadleaf forests flanking the Westland gap and its absence in the gap may be related to incomplete recolonization following glacial retreat. We also discuss species status and an ancient polymorphism within *B. scutellaris*.

Keywords: coalescence dating, coalescent analysis, nested clade analysis, New Zealand biogeography, *Nothofagus* gap, Pleistocene, refugia

Received 5 July 2007; revision received 3 September 2007; accepted 1 November 2007

Introduction

The 'beech gap' in central Westland, South Island, New Zealand (Fig. 1), has been under scrutiny for years because *Nothofagus* trees (Fagaceae), one of the dominant New Zealand forest species, are noticeably absent from this area (Cockayne 1926; Wardle 1963; Burrows 1965). Forests in the gap are plentiful but are dominated by podocarps and broadleaf species and the Westland beech gap is contiguous with a larger beech gap area that ranges through mixed altitudes and climate regimes (McGlone *et al*. 1996); however, it is the Westland beech gap that has attracted the most attention from biologists. There are four species of *Nothofagus* in New Zealand, and they form the bulk of montane and subalpine tree line forests throughout New Zealand and are common in lowland forests in the South Island. Cockayne (1926, 1928) was the first to comment on a spectacular sea-to-mountain crest absence of beech species from 150 km of central Westland, South Island. Cockayne noted that this beech gap coincided with the region where the glaciers of the Last Glacial Maximum (LGM, 34 000–18 000 years ago) surged out beyond the present coastline and suggested that the complete

Correspondence: Richard A. B. Leschen, Fax: 64-9-574-4101; E-mail: leschenr@landcareresearch.co.nz

© 2008 Landcare Research
Journal compilation © 2008 Blackwell Publishing Ltd

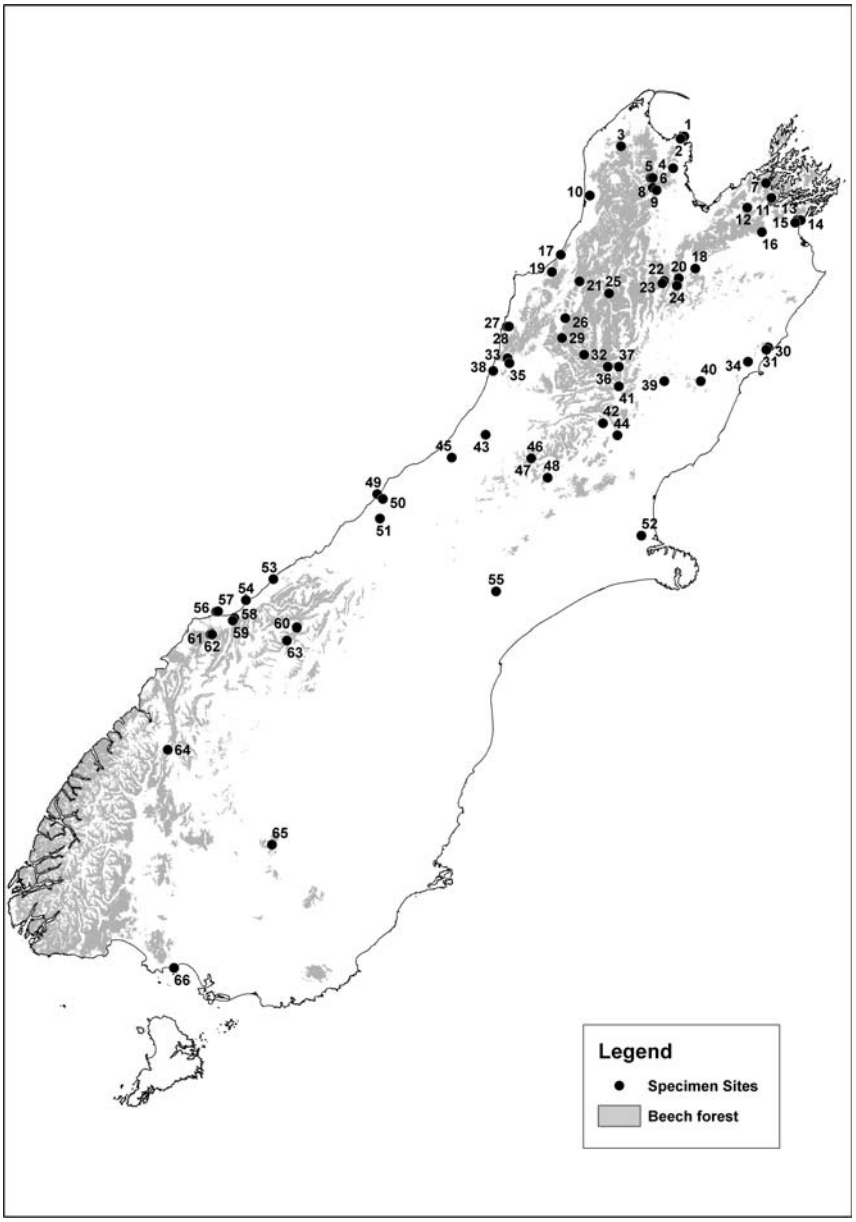

Fig. 1 Distribution of *Nothofagus* forest in the South Island of New Zealand, including forests containing broadleaf and podocarp species. Localities are numbered and cross-referenced in Table 1.

extirpation of beech species at that time was responsible for the present-day absence. This became the standard explanation for the beech gap (Wardle 1963; Burrows 1965), a community phenomenon that effects the distribution of plants (Haase 1990) and animals (McDowall 1997, 2005; Leschen & Michaux 2005).

Nevertheless, McGlone (1985) noted there are certain features of the beech gap that are difficult to explain by a simple glacial ice hypothesis. First, there was extensive ice coverage to the south of the beech gap and lesser, but still highly significant, valley glaciation to the north. Therefore, the beech gap does not neatly correspond with any set of glacial features. Second, the beech-free podocarp-broadleaf forests of the gap are similar to those that were dominant north and south of the gap at the end of the LGM but were invaded and partially replaced by beech in the course of the Holocene. Absence of beech in central Westland has therefore been secondarily attributed to the slow invasive rate of beech species when they are totally absent from a region, and the lack of suitable invasion routes in the mountainous terrain (Wardle 1964; Burrows 1965; Wardle *et al*. 1988). McGlone (1985) and Haase (1990) argued that edaphic and climatic factors — namely, more fertile soils and milder climates of the central zones — were the primary reasons for the exclusion of beech.

More recent work has confirmed that environmental factors are insufficient to exclude beech from the central Westland lowlands or prevent its dominance in the montane/

© 2008 Landcare Research
Journal compilation © 2008 Blackwell Publishing Ltd

subalpine zone (Leathwick 1998; Hall & McGlone 2006). Hall & McGlone (2006) further suggested that a low level of forest stand disturbance in central Westland could also play a role in making it difficult for the relatively short-lived beech to invade long-lived podocarp forest tracts. The consensus now is that the primary reason for the beech gap is LGM glaciation, but that the combination of unfavourable terrain for beech invasion and suitability of the lowland environment for competing podocarp-angiosperm forest is the reason beech continues to be absent (McGlone *et al*. 1996). Given the 2 million plus years that glaciation has been a repetitive feature of the Southern Alps (Suggate 1990), separation of taxa by the effects of ice could have taken place at any time within this period. Also, it has been argued that infrequent long-distance dispersal across the Westland gap is one possible reason for split distributions (Wardle *et al*. 1988).

We examine the origin and maintenance of the beech gap by reconstructing the population histories of two species of fungus-feeding microcoleoptera, a rove beetle [*Brachynopus scutellaris* (Redtenbacher), Staphylinidae, Scaphidiinae, Scaphisomatini, Fig. 2(A)] and a sap beetle [*Hisparonia hystrix* (Sharp), Nitidulidae, Nitidulinae, Fig. 2(B)]. Both species are very widely distributed and found in all forest types in New Zealand but *H. hystrix* is found through the beech gap while *B. scutellaris* extends only a short distance into the gap. We use population genetic and phylogenetic analysis of mitochondrial DNA (mtDNA) coupled with information on natural history to reconcile historical and ecological hypotheses on beech gap origin and maintenance.

The mechanisms we discussed above make a variety of predictions regarding the expected patterns of genetic variation in species both present and absent in the gap. If glacial ice distribution is the major reason for the absence of taxa within the Westland gap, lineage splits should be young, as other environmental features should not have been an insurmountable barrier to distributions reforming across the gap given the thousands of years the gap remains ice-free between glacial maxima. For example, a recent vicariant origin of the beech gap could predict a lack of reciprocal monophyly of populations to the north and south of the beech gap. However, if there is a strong environmental component to a given absence, such as the proposed inability of beech to compete with pre-existing podocarp dominant associations, lineage splits could be older. A more ancient origin predicts that one or both of these populations may be monophyletic. Alternatively, a long-distance dispersal event across the gap should be detectable using a method such as nested clade analysis (NCA; Templeton *et al*. 1995). For species like *H. hystrix* that are distributed through the gap, these may exhibit a pattern of genetic admixture, indicating recent gap closure, or may possess unique haplotypes suggestive of long-term *in situ* survival. These hypotheses can also be addressed by the application of molecular dating methods (e.g. Buckley *et al*. 2001a), and here we use coalescence and isolation/migration models to estimate gene and population divergence times.

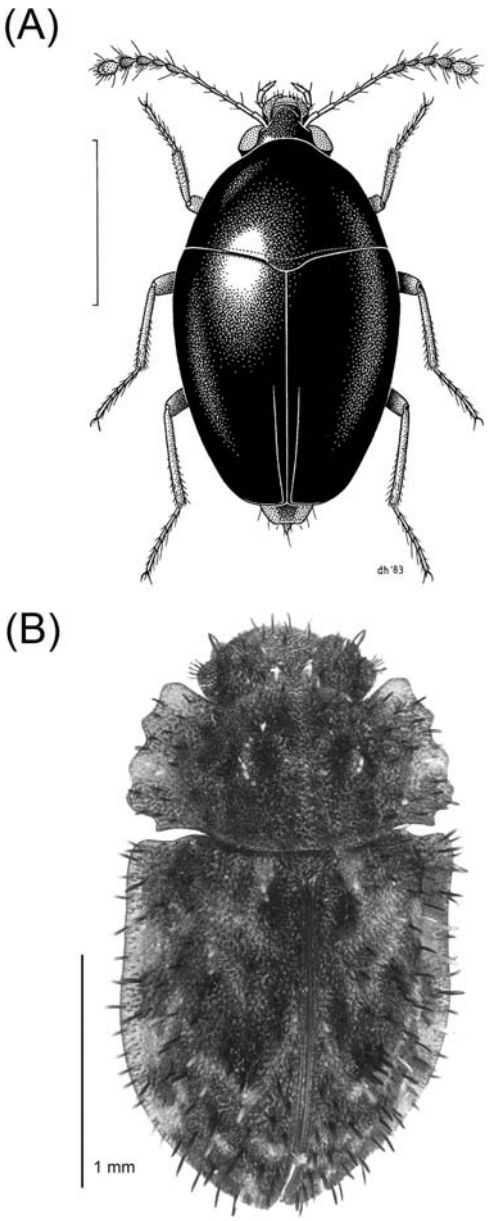

Fig. 2 Habitus illustration of (A) *Brachynopus scutellaris* and automontage photograph of (B) *Hisparonia hystrix*. Scale bars = 1 mm.

Methods

Taxon sampling

Brachynopus scutellaris and *Hisparonia hystrix* were chosen as model species because they are very widely distributed in New Zealand, occurring on New Zealand's main islands

© 2008 Landcare Research
Journal compilation © 2008 Blackwell Publishing Ltd

(Löbl & Leschen 2003a; Carlton & Leschen 2007). Both are members of endemic New Zealand genera. *B. scutellaris* is one of two species in its genus (the other is the North Island species, *Brachynopus latus* Broun), and the genus *Brachynopus* Broun is placed in a basal position in the tribe Scaphisomatini based on adult morphology (Leschen & Löbl 2005). *Hisparonia hystrix*, a member of a monotypic genus, is related to members of the informal *Soronia* group in the Nitidulinae (Kirejtshuk 2003; Carlton & Leschen 2007). Both *B. scutellaris* and *H. hystrix* are fungus-feeding, but on very different fungi and in different habitats. *B. scutellaris* is found on polypore fungi, mainly resupinate forms found beneath rotting logs (Löbl & Leschen 2003a) and in beech and podocarp forest habitats with well-developed leaf litter and dead wood. *H. hystrix* is found exclusively on sooty moulds which are a significant (and unusual) component of the New Zealand forests (Hughes 1976). Sooty moulds grow on trees that support *Ultracoelostoma* (Hemiptera, Margarodidae) and other coccids that secrete honey-drew upon which the fungi thrive. Principal tree hosts include mainly *Nothofagus* and *Leptospermum scoparium* (Ericaceae), but there are several other hosts that *H. hystrix* has been recorded from (Carlton & Leschen 2007).

Specimens of *H. hystrix* were collected by beating shrubs with sooty moulds. *B. scutellaris* was collected by hand from dead wood with host fungal growth or by sifting dead wood, host fungi and leaf litter. The study is based on 113 samples of *B. scutellaris* from the South Island (Table 1) and two specimens from Auckland (37°00′S, 174°33′E) and 105 samples of *H. hystrix* (Table 1). Distributions were described and mapped using the LENZ environmental mapping tool (Leathwick *et al*. 2003) in ArcGIS.

Laboratory methods

Beetles were stored in 95% ethanol at –20 °C. Total genomic DNA was extracted from entire beetles using the QIAGEN DNeasy Tissue Kit. The 3-h lysis step was followed by a 1-h RNase treatment at 55 °C. DNA was resuspended in AE buffer and stored at 4 °C. DNA concentration was determined by spectrophotometry. The 3′ end of the mitochondrial cytochrome oxidase subunit I (COI) gene region (approximately 820 bp) was amplified using the primers C1-J-2195 and TL2-N-3014 (Simon *et al*. 1994). Polymerase chain reaction (PCR) was performed in 50 μL reactions containing 2 μL DNA template, 4 μM each primer, 0.2 mM dNTPs, 0.625 mM $MgCl_2$ and 2.5 U Ampli*Taq* Gold in 1× buffer. The procedure was carried out on an Applied Biosystems GeneAmp PCR System 9700 thermo cycler using the following protocol: 5 min at 95 °C, 5 min; 30 cycles of 1 min at 94 °C, 1 min at 56 °C, 1.5 min at 72 °C; 10 min at 72 °C. PCR fragments were purified using Roche High Pure PCR Product Purification Kit. Fluorescence-based sequencing was conducted on the purified PCR templates in both directions using ABI PRISM Big Dye version 3.1 (Applied Biosystems) with unincorporated dye labels removed by ethanol precipitation. Sequence data were collected on an ABI PRISM 3100-Avant Genetic Analyser and edited using SEQUENCHER 3.1.1. Sequence alignments were made using CLUSTAL_X (Thompson *et al*. 1994).

Phylogenetic analysis

The best-fit model from the set of candidate models was selected using the Akaike information criterion (AIC; Akaike 1973; Posada & Buckley 2004) as implemented in PAUP*4.0 in conjunction with MODELTEST 3.0 (Posada & Crandall 1998). We performed model selection on ML trees estimated under the model of Jukes & Cantor (1969). Maximum-likelihood tree searches utilized 10 starting trees obtained by stepwise addition with random addition sequence and tree-bisection–reconnection branch-swapping (Swofford 1998). Preliminary analyses suggested that rooting the gene trees with sister-species outgroups was problematic due to the extreme genetic distance between the ingroups and outgroups, and therefore, trees were rooted under the molecular clock assumption. Summary statistics were calculated using DNASP version 4.10.7 (Rozas *et al*. 2003).

Coalescent analyses

Coalescent analyses were performed in a Bayesian framework using Markov chain Monte Carlo (MCMC). Bayesian hypothesis testing was performed using the Bayes factor (e.g. Kass & Raftery 1995). We calculated the harmonic means of the marginal likelihoods and then estimated the Bayes factor as described by Newton & Raftery (1994) and Nylander *et al*. (2004). We used this approach to choose between models of population growth and constant population size. We also tested the assumption of the molecular clock by calculating the Bayes factor for a strict clock model and an uncorrelated exponential model (Drummond *et al*. 2006). For the molecular clock analyses, we used two rates, one described by Brower (1994) for arthropod mitochondrial DNA of 0.023 substitutions/site/million years, which corresponds to a rate of 0.0115 from the root to the tips of the tree (per lineage). The second rate of 0.015 substitutions/site/million years for the insect COI gene was obtained from Quek *et al*. (2004) and corresponds to a rate of 0.007 from the root to the tips.

We performed three sets of analyses to estimate gene and population divergence times and patterns of population size change. The first analyses were performed using the program BEAST 1.4 (Drummond & Rambaut 2006). For the coalescent models, we performed analyses under both constant population size and exponential growth models (e.g. Kuhner *et al*. 1998; Drummond *et al*. 2002). We used the following prior distributions: general time reversible

© 2008 Landcare Research
Journal compilation © 2008 Blackwell Publishing Ltd

Table 1 Locality information for taxa in this study. Locality and number of specimens for haplotypes of *Brachynopus scutellaris* (haplotypes 1–73). Locality and number of individuals for haplotypes of *Hisparonia hystrix*

Site no.	Locality	Latitude/longitude	*Brachynopus scutellaris* haplotype (*n*)	*Hisparonia hystrix* haplotype (*n*)
1	Totoranui	40°49′S, 173°00′E	—	14(2)
2	Pigeon Saddle	40°50′S, 172°58 E	33(1), 34(1), 62(2)	—
3	Brown Hut	40°53′S, 172°26′E	61(1)	14(1), 15(1)
4	Riwaka Scenic Reserve	41°02′S, 172°54′E	60(1)	8(1), 14(1)
5	Cobb Valley Ridge	41°06′S, 172°42′E	—	16(1), 40(3)
6	Asbestos Track	41°06′S, 172°43′E	8(1), 10(1)	—
7	Bridle Track	41°08′S, 173°44′E	1(1)	—
8	Mount Arthur (A)	41°10′S, 172°43′E	7(1), 9(1)	—
9	Mount Arthur (B)	41°11′S, 172°45′E	—	40(1), 41(1)
10	Oparara Gorge	41°13′S, 172°09′E	11(4)	—
11	Nydia Track	41°14′S, 173°47′E	3(1), 4(1)	—
12	Pelorus Bridge	41°18′S, 173°34′E	2(1), 6(1), 12(2)	—
13	Pukaka Valley Walk (A)	41°23′S, 174°01′E	4(2)	—
14	Rarangi	41°23′S, 174°03′E	—	14(1)
15	Pukaka Valley Walk (B)	41°24′S, 174°00′E	—	29(3)
16	Onamalutu Sc. Reserve	41°28′S, 173°42′E	4(1), 5(1)	—
17	Charming Creek Walk	41°37′S, 171°53′E	11(1), 14(1), 41(1)	—
18	Kowhai Point Reserve	41°43′S, 173°06′E	—	2(1), 5(1)
19	Denniston Saddle	41°44′S, 171°48′E	41(1), 47(1), 50(1)	43(2)
20	Rainbow Homestead	41°47′S, 172°57′E	—	—
21	Lyell Walkway	41°48′S, 172°03′E	49(1), 51(1)	—
22	Lake Rotoiti	41°48′S, 172°49′E	—	7(1), 14(1)
23	Mount Robert	41°49′S, 172°48′E	58(1), 64(1)	43(2)
24	Dip Flat	41°50′S, 172°56′E	35(2)	7(1), 43(1)
25	Murchison (20 km south)	41°53′S, 172°19′E	40(1), 41(1)	14(3)
26	Boatmans Creek	42°03′S, 171°55′E	48(1)	14(1)
27	Bullock Creek	42°06′S, 171°23′E	—	47(1), 48(1), 49(2)
28	Cave Creek Monument	42°06′S, 171°24′E	11(3), 15(1), 16(1), 17(1), 18(1), 19(1)	44(1), 45(1)
29	Alborn Coal Mine	42°11′S, 171°53′E	—	43(2)
30	Seaview Scenic Reserve	42°15′S, 173°46′E	68(1), 69(1)	4(1), 7(1)
31	Puhipuhi Reserve	42°16′S, 173°45′E	—	1(1), 7(1), 14(2)
32	Rahu Reserve	42°18′S, 172°05′E	41(1), 42(1)	13(1)
33	Croesus Track	42°19′S, 171°23′E	—	34(1), 36(1), 46(1)
34	Mount Fyffe	42°21′S, 173°35′E	58(2), 59(1)	14(2)
35	Blackball	42°21′S, 171°24′E	39(1), 44(1), 45(1), 46(1)	32(1)
36	Maruia Springs	42°23′S, 172°18′E	41(2)	43(1)
37	Lewis Pass	42°23′S, 172°24′E	38(1), 41(1)	—
38	Coal Creek Walk	42°24′S, 171°15′E	—	33(1), 34(1)
39	Jacks Pass	42°29′S, 172°49′E	36(2)	9(1), 10(1)
40	Mount Lyford	42°29′S, 173°09′E	67(1)	7(1), 14(1)
41	St. James Walkway	42°31′S, 172°24′E	37(1), 38(3)	3(1), 4(1), 7(1)
42	Lake Taylor	42°46′S, 172°15′E	13(2)	6(1)
43	Lake Kanieri	42°50′S, 171°10′E	43(1)	34(2), 35(1)
44	Hurunui R (South Br)	42°51′S, 172°23′E	—	14(2)
45	Totara Saddle Forest	42°59′S, 170°51′E	—	21(1), 37(2), 38(1), 39(1)
46	Klondyke Corner	43°00′S, 171°35′E	63(2)	37(1), 38(1)
47	Bealey Hotel	43°00′S, 171°35′E	—	11(1), 14(1)
48	Craigieburn	43°08′S, 171°44′E	—	12(1), 14(2)
49	Okarito Trig Walk	43°13′S, 170°09′E	—	17(1), 18(1), 19(1), 24(1)
50	Pakihi Track	43°15′S, 170°12′E	—	18(3), 21(1)
51	Franz Josef Glacier	43°23′S, 170°10′E	—	20(1), 22(1), 23(1), 25(1), 42(1)
52	Riccarton Bush	43°32′S, 172°36′E	66(2)	—
53	Ship Creek	43°46′S, 169°09′E	28(1), 29(1), 30(1), 31(1)	—
54	Hapuka Estuary	43°54′S, 168°53′E	—	14(1)

© 2008 Landcare Research
Journal compilation © 2008 Blackwell Publishing Ltd

Table 1 *Continued*

Site no.	Locality	Latitude/longitude	*Brachynopus scutellaris* haplotype (*n*)	*Hisparonia hystrix* haplotype (*n*)
55	Peel Forest	43°54′S, 171°14′E	65(1)	—
56	Wharekai Walk	43°58′S, 168°36′E	21(1), 23(1), 26(1), 27(1)	—
57	Jacksons Bay Track	43°58′S, 168°37′E	20(1), 22(1), 24(1), 25(1)	—
58	Mount McLean	44°01′S, 168°46′E	52(1), 54(1), 55(1), 56(1), 57(1)	—
59	Sponge Swamp	44°02′S, 168°45′E	—	14(3)
60	Haast Pass	44°06′S, 169°21′E	52(1)	—
61	Red Hills	44°07′S, 168°32′E	—	26(3), 27(1), 28(1)
62	Martyr Saddle	44°07′S, 168°33′E	21(2)	—
63	Brady Creek	44°11′S, 169°15′E	52(3), 53(1), 70(1), 71(1), 72(1)	—
64	Eglinton Valley	44°53′S, 168°04′E	32(2)	—
65	Piano Flat	45°34′S, 169°01′E	63(2)	—
66	Mores Scenic Reserve	46°22′S, 168°00′E	—	—
67	Lake Waikaremoana (NI)	38°48′S, 177°07′E	—	30(1)
68	Waipoua St Forest (NI)	35°37′S, 173°33′E	—	31(1)

(GTR) model rate matrix (exponential, mean = 1), alpha shape parameter (exponential, mean = 1), proportion of invariable sites (uniform, 0–1), exponential and constant population size parameters (uniform, 0–2.8), exponential growth rate parameter (uniform, -1×10^6–1×10^6), and tree height (exponential, mean = 10 or 25). We used a rather informative prior for the tree height (tree root), and varied this prior, because the haplotypes are very closely related and recent studies have shown that overly vague priors on branch lengths can result in misleading inferences (Yang & Rannala 2005). An exponential prior with a mean of 25 places most weight on tree heights of less than 0.1 and a mean of 10 places most weight on tree heights of less than 0.3. Maximum-likelihood estimates of the tree height were less than 0.1, indicating that these highly informative priors encompassed the ML estimate. We initially performed short MCMC runs of 5×10^6 cycles in order to select the burn-in length, to optimize values for the MCMC proposal and tuning parameters, and to ensure that mixing was adequate. We then repeated these analyses for $30–40 \times 10^6$ cycles with a thinning interval of 10 000. This ensured that the ESS values for all parameters were greater than 1000. These analyses were applied to both of the target species and yielded date estimates for the time to most recent common ancestor (TMRCA) of a specified clade. The sampling of trees is performed by BEAST, and therefore, we used the posterior probabilities of individual nodes as a measure of nodal support.

For the second set of analyses, we applied the Bayesian skyline method (Pybus *et al*. 2000; Drummond *et al*. 2005) as implemented in BEAST 1.4 (Drummond & Rambaut 2006) for reconstructing the timing and magnitude of population size changes. We used the same substitution models, prior distributions, and MCMC settings as described above with the addition of a uniform prior on the skyline population size (0–70). The Bayesian skyline analyses were applied to both species.

The third set of analyses was the isolation/migration model (IM model) of Neilsen & Wakeley (2001) as implemented in the program MDIV (Neilsen & Wakeley 2001), which we used to date the divergence between populations to the north and south of the beech gap for *B. scutellaris*. The IM model allows the joint estimation of migration rates, population size, and divergence times. For pairs of panmictic populations (1 and 2) and their ancestral population (A), this model estimates asymmetric migration rates between two populations (m_1 and m_2), population mutation rates (θ_1, θ_2, θ_A), and time since population splitting (t). We constrained the model such that $\theta_1 = \theta_2 = \theta_A$, and $m_1 = m_2$ in order to reduce the computational complexity to an acceptable level. Likelihood calculations were performed under the HKY85 model (Hasegawa *et al*. 1985). Because our initial analyses with vague priors indicated that m was close to zero, and because the gene trees showed no sharing of haplotypes between populations north and south of the beech gap, we fixed m to be 0. By fixing this parameter, we were also able to obtain marginal distributions on t that were well constrained within the boundaries of what we consider to be realistic priors. This was not the case when we estimated both m and t, where the distribution appeared to have no upper bound, possibly due to the model being overparametized. We used uniform priors on the divergence time (0–50), transition/transversion ratio (0–100), and theta (0–30.6). We assumed a generation time of 1 month for *B. scutellaris* (unpublished observations) in order to convert the divergence times to years. We ran a single MCMC chain for 1×10^7 cycles, with a burn-in of 1×10^6 cycles. This analysis was repeated four times and marginal distributions were compared across analyses to check for convergence.

© 2008 Landcare Research
Journal compilation © 2008 Blackwell Publishing Ltd

Because our preliminary analyses indicated that *H. hystrix* is a continuously distributed population through the beech gap, the IM model was not applied to those data.

Nested clade analysis

We used NCA (Templeton *et al*. 1995) to investigate the association between geographical and genetic variation and to infer the processes responsible. For each species, we first constructed a haplotype network using TCS version 1.21 (Clement *et al*. 2000) according to the acceptance criteria outlined in Templeton *et al*. (1992). We treated evolutionary ambiguities, expressed as reticulate connections in the haplotype network, according to the criteria in Crandall & Templeton (1993). Clades within the inferred networks were nested into hierarchically interlocking groups using standard nesting rules (Templeton *et al*. 1987; Templeton & Sing 1993; Templeton 1998). The nested clade design and a pairwise distance matrix were used by GEODIS 2.4 (Posada *et al*. 2000) to calculate the following statistics (Templeton 1998): clade distance (D_c), a measure for the geographical range of a particular clade; nested clade distance (D_n), which measures the geographical range of a clade relative to its closest sister clades; intertip distances (I-T_c and I-T_n), which indicate how widespread younger clades (tips) are compared to their ancestors (interiors), relative to other clades within the same nesting clade. Inferences about population processes were made, using inference keys (Templeton *et al*. 1995; Templeton 1998; http://darwin.uvigo.es/software/geodis.html, November 2005), for any clades that showed statistically significant geographical association of haplotypes.

Results

Patterns of DNA sequence variation and population size

We sequenced a total of 113 and 105 individuals of *Brachynopus scutellaris* and *Hisparonia hystrix*, respectively (Table 1). All sequences have been submitted to GenBank under Accession nos EU145025 to EU145243. *B. scutellaris* had a higher level of sequence variation than *H. hystrix*, with 73 haplotypes compared to 47 and 98 segregating sites compared to 45. Tajima (1989) *D* values were both negative, but not significantly so, suggesting that the data are conforming to neutral expectations. The best-fit model for the *B. scutellaris* data set was GTR + I + Γ (Lanave *et al*. 1984; Yang 1994; Gu *et al*. 1995) and the best-fit model for the *H. hystrix* data set was HKY85 + I. The posterior probability distributions of the proportion of invariable sites, α shape parameter for among-site rate variation, and GTR rate matrix parameters, obtained from the BEAST analyses, indicate strong transition bias and among-site rate variation, consistent with other studies of insect mtDNA (e.g. Buckley *et al*. 2001b).

We subdivided the *H. hystrix* data into individuals sampled from within the beech gap and those sampled outside the beech gap. Outside the gap, there were 83 individuals and 34 haplotypes, with a haplotype diversity of 0.892 (s.d. = 0.027). Inside the gap, there were 23 individuals and 15 haplotypes, giving a haplotype diversity of 0.953 (s.d. = 0.027). Therefore, despite the much smaller geographical range encompassing the within beech gap samples, there is a higher level of genetic diversity.

We tested the assumption of a molecular clock by estimating the Bayes factor between the strict clock and the uncorrelated exponential model. For the *H. hystrix* data, the Bayes factor was 3.212, which corresponds to 'positive' support for the nonclocklike model. For the *B. scutellaris* data, the Bayes factor was 12.295, indicating 'very strong' support for the nonclocklike model. Therefore, the data appear to be evolving in a nonclocklike manner.

The Bayes factor analyses indicated that both data sets fitted a model of exponential population growth much better than a constant population size model (Table 2). Furthermore, for both species the 95% credible intervals on the exponential growth rate parameter, *r*, exclude zero, consistent with an increasing population size (Table 2). The Bayesian skyline plots for both species are also consistent with a recent population expansion (Fig. 6).

Gene tree topology

The mtDNA gene tree for *B. scutellaris* contains four deeply diverging lineages each with well-supported monophyly (Fig. 3). We have named these clades 'Brady Creek', 'Eastern', 'A-clade' and 'B-clade'. The outgroup sequences were too divergent to reliably root the gene trees; therefore, we estimated the position of the root using Bayesian inference under the assumption of a strict molecular clock (e.g. Huelsenbeck & Imennov 2002). For *B. scutellaris*, the root of the gene tree lies between the Eastern clade and the remaining three major clades. The A-clade and B-clades of *B. scutellaris* contain three subclades each with a similar geographical distribution, which we have termed the 'Northeast', 'Southern' and 'Northern' subclades. The Southern subclades are distributed in Westland south of the beech gap and into Fiordland. The Northern subclades are distributed north of the beech gap. In both the A- and B-clades, the Southern subclades are nested within the Northern subclades. The Northeast subclade in the A-clade is paraphyletic, but this is poorly supported. The Northeast subclade in the B-clade is monophyletic and sister group to the Southern + Northern subclades.

The Brady Creek clade is represented by a limited sample of individuals from two geographically separated populations, at Brady Creek in the southern South Island and at Auckland in the north of the North Island. The Eastern

© 2008 Landcare Research
Journal compilation © 2008 Blackwell Publishing Ltd

Table 2 Sequence statistics and marginal distributions of model parameters

	Hisparonia hystrix	*Brachynopus scutellaris*
No. of individuals	105	113
No. of sites	787	786
Segregating sites	45	98
No. of varied sites	45	100
No. of parsimony informative sites	26	88
Tajima's *D*	–1.26188 ($P > 0.1$)	–0.02593 ($P > 0.1$)
No. of haplotypes	47	73
Nucleotide diversity per site (π)	0.00684 (0.00033)	0.02739 (sd = 0.0011)
Haplotype diversity	0.93 (sd = 0.018)	0.983 (sd = 0.005)
Average number of nucleotide differences	5.37	21.53
Best AIC model	HKY85 + I	GTR + I + Γ
rAC	—	1.000
rAG	—	21.476
rAT	—	0.220
rCG	—	0.220
rCT	—	8.489
rGT	—	1.000
ts/tv	18.047	—
α		0.871
p_{inv}	0.901	0.803
Frequency of A	0.328	0.317
Frequency of C	0.148	0.172
Frequency of G	0.144	0.130
Frequency of T	0.379	0.381
Marginal likelihood: constant size	–135.0954	–197.7428
Marginal likelihood: exponential growth	–65.2834	–167.4499
Bayes factor	8.49 ('strong')	6.82 ('strong')
Exponential growth rate (*r*)	22.525 (8.844–39.284)	1.931 (0.498–3.454)

clade is distributed from Northeast Marlborough, down the east coast of the South Island and into Central Otago.

As for *B. scutellaris* data, we used a Bayesian implementation of the molecular clock to root the *H. hystrix* gene tree (Fig. 4). This method placed the root between haplotypes sampled from the North Island, Northeast Marlborough and Westland and all other remaining South Island haplotypes. The *H. hystrix* gene tree contains less geographical structure; however, several major clades are evident, with high posterior probabilities (Fig. 4). Individual haplotypes sampled from within the beech gap are distributed across several clades and so do not form a monophyletic group. Several haplotypes sampled from within the beech gap are unique to the gap, although they tend to be closely related to haplotypes found immediately to the north or south of the gap.

Dates of divergence

We used three methods for dating population divergences in *B. scutellaris*. The first method was to infer the age of populations by estimating the TMRCA of specified haplotype lineages. We used this method to directly date the age of the split between the Northern and Southern clades on either side of the beech gap. For *B. scutellaris*, the divergence of the Southern and Northern A- and B-clades is 224 000–926 000 years ago and 222 000–925 000 years ago, respectively (Table 3). Using the more constrained prior on the tree height with an exponential mean of 25 caused the marginal distributions on TMRCA to decrease as did using a slower substitution rate. These dates are well within the Pleistocene, which began approximately 2.5 million years ago. The second method was using the IM model (Neilsen & Wakeley 2001), which yields estimates of actual population divergence times rather than haplotype divergence times. These analyses yielded divergence dates of 70 771 years (95% Bayesian credible intervals of 42 346–113 118) with the fast rate of 0.0115, and 116 267 years (95% Bayesian credible intervals of 69 569–185 836) with the slow rate of 0.007 (Fig. 5). Under both rate assumptions, we can exclude population divergence dates less than approximately 40 000 years. All of these dates precede the LGM which spans 17 650–34 000 BP (Suggate & Almond 2005). However, both of these estimates used an average generation time of 2 months. If we were to assume a faster generation time, then the dates would become more recent.

© 2008 Landcare Research
Journal compilation © 2008 Blackwell Publishing Ltd

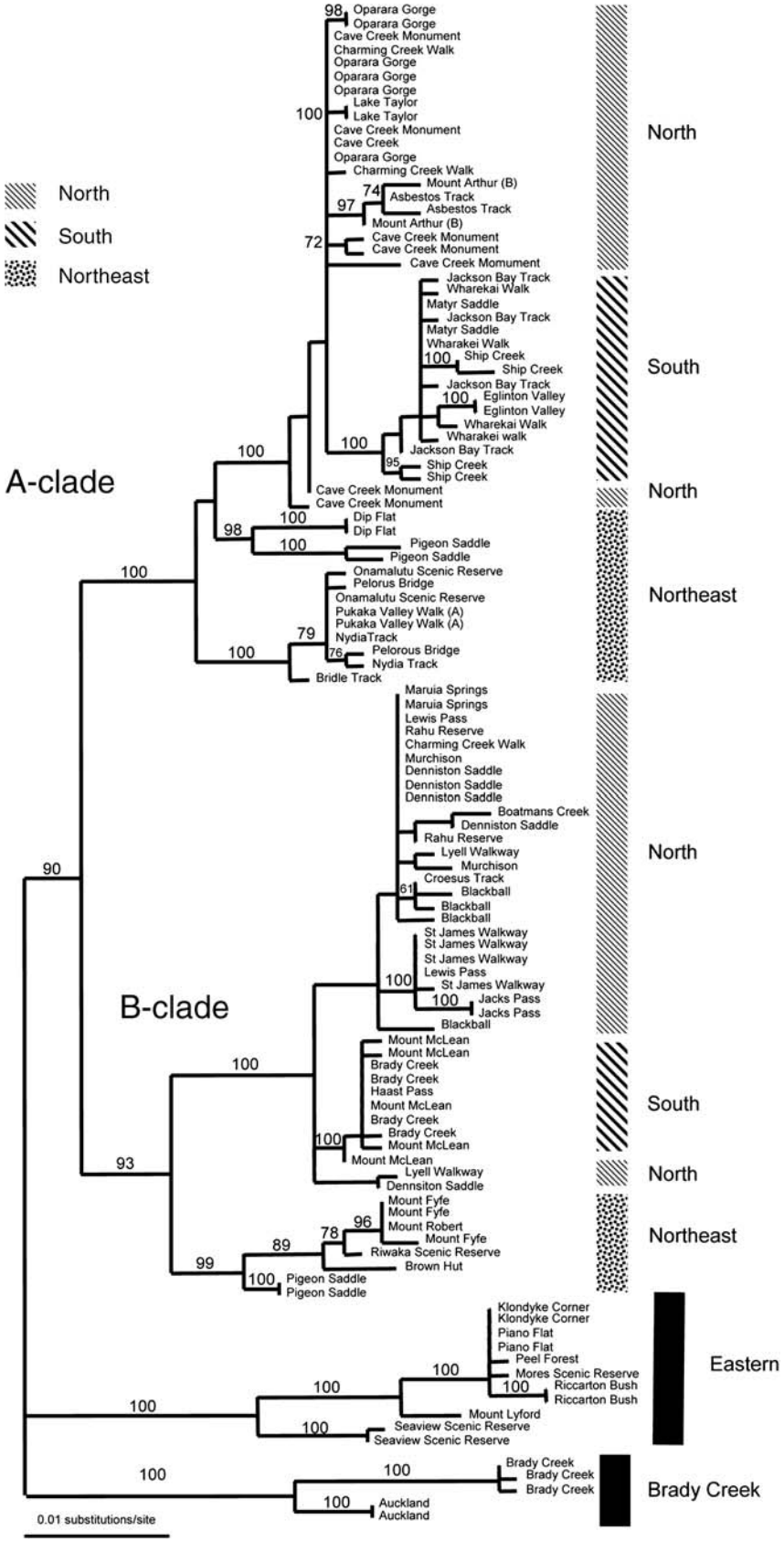

Fig. 3 Maximum-likelihood gene tree for *Brachynopus scutellaris*. Branch lengths are drawn proportional to the expected number of substitutions per site. Numbers above nodes are posterior probabilities expressed as percentages. Major clades are indicated with vertical patterned bars.

© 2008 Landcare Research
Journal compilation © 2008 Blackwell Publishing Ltd

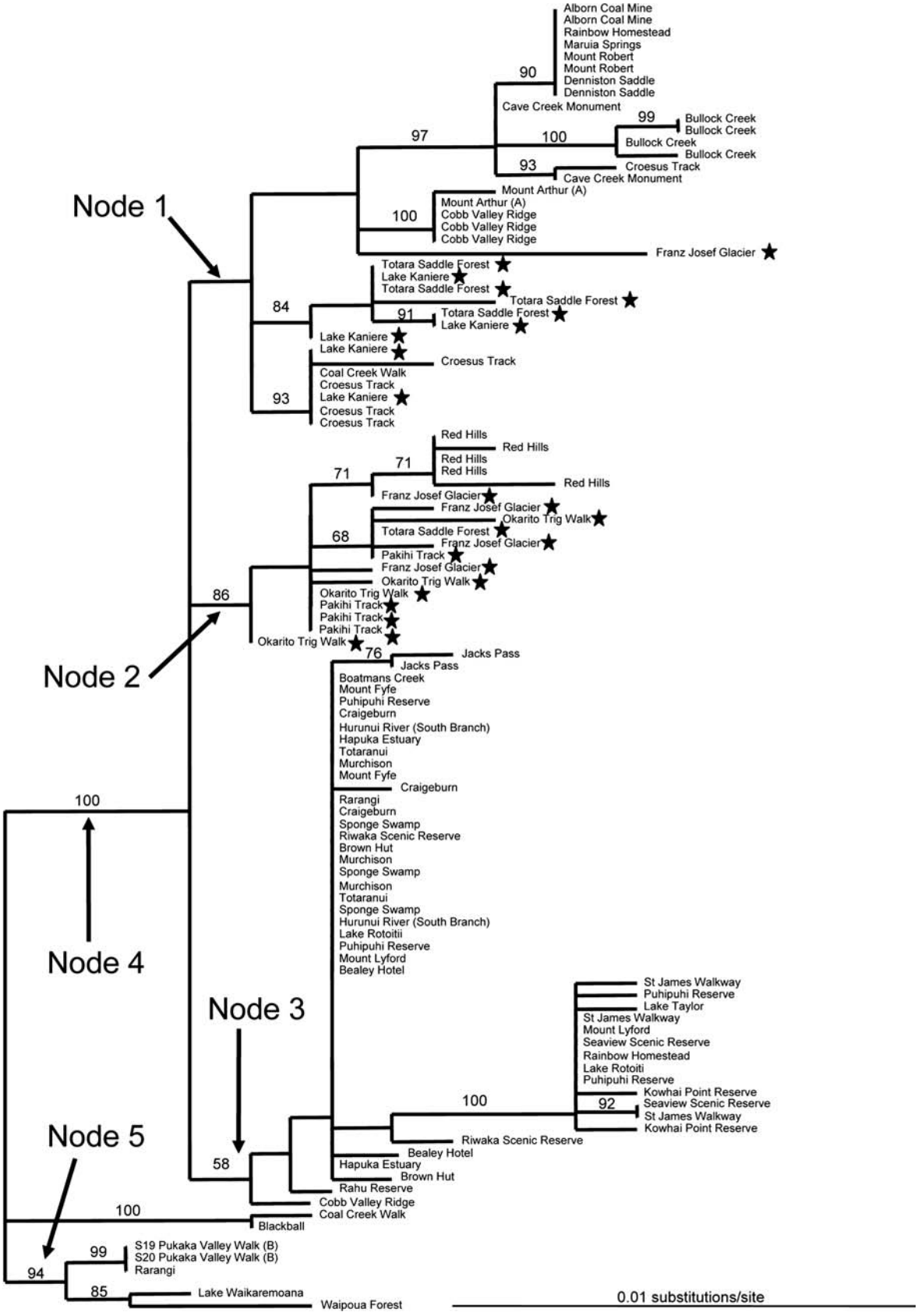

Fig. 4 Maximum-likelihood gene tree for *Hisparonia hystrix*. Branch lengths and nodal support values are represented as in Fig. 3 and the stars indicate localities within the beech gap. Major clades are numbered from 1 to 5.

Table 3 Dates of time to most recent common ancestor (TMRCA) for *Brachynopus scutellaris* data

	Rate = 0.023 Height = exp(25)	Rate = 0.023 Height = exp(10)	Rate = 0.015 Height = exp(25)	Rate = 0.015 Height = exp(10)
South_A	0.375 (0.220–0.542)	0.465 (0.272–0.678)	0.509 (0.295–0.727)	0.651 (0.370–0.926)
North_A	0.265 (0.148–0.428)	0.322 (0.174–0.507)	0.365 (0.194–0.562)	0.457 (0.240–0.711)
South_north_A	0.378 (0.224–0.542)	0.470 (0.261–0.665)	0.514 (0.304–0.727)	0.658 (0.384–0.926)
NE_A	0.673 (0.429–0.929)	0.855 (0.552–1.22)	0.886 (0.592–1.230)	1.181 (0.748–1.666)
Brachy_A	0.689 (0.474–0.950)	0.878 (0.564–1.204)	0.907 (0.609–1.226)	1.218 (0.796–1.666)
South_B	0.111 (0.038–0.202)	0.131 (0.047–0.234)	0.156 (0.053–0.275)	0.185 (0.068–0.324)
North_B	0.350 (0.201–0.504)	0.434 (0.247–0.633)	0.478 (0.277–0.679)	0.609 (0.341–0.870)
North_south_B	0.364 (0.222–0.529)	0.449 (0.257–0.643)	0.496 (0.304–0.699)	0.631 (0.388–0.925)
Brachy_B	0.906 (0.556–1.281)	1.214 (0.668–1.702)	1.172 (0.744–1.602)	1.648 (1.045–2.409)
East	0.693 (0.414–0.967)	0.954 (0.551–1.360)	0.875 (0.537–1.224)	1.273 (0.755–1.822)
Auck_Brady	0.500 (0.269–0.736)	0.687 (0.343–1.022)	0.640 (0.348–0.953)	0.916 (0.492–1.401)
Brachy_A_B	1.217 (0.896–1.573)	1.683 (1.145–2.185)	1.538 (1.122–1.953)	2.249 (1.568–2.943)
Tree height	1.452 (1.127–1.788)	2.210 (1.677–2.829)	1.768 (1.377–2.160)	2.818 (2.154–3.541)

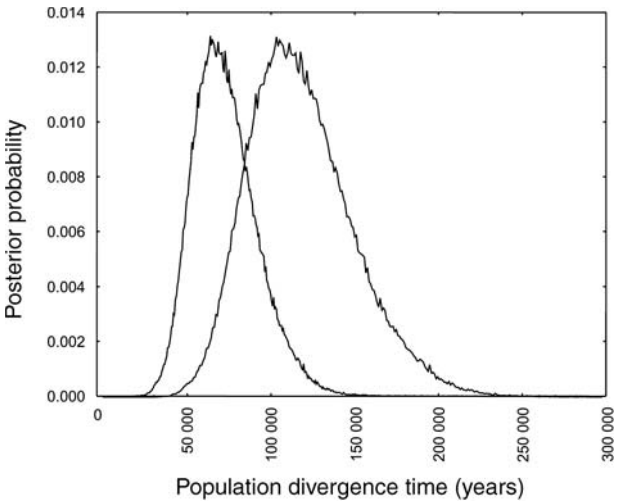

Fig. 5 Marginal distributions for IM results under fast (A) and slow (B) substitution rate assumptions. The solid lines show the mean posterior values for the population size through time and the dotted lines show the 95% credible intervals.

The third dating method we implemented was the Bayesian skyline plot (Drummond *et al*. 2005), which we used to date shifts in population size using the entire *B. scutellaris* gene tree. Using a prior of 25 on the tree height and a rate of 0.0115, the *B. scutellaris* curve shows evidence for a long-term gradual increase in population size, followed by a decline somewhere between 200 000 and 50 000 years ago (Fig. 6). Immediately after the population size reached its lowest level, the population size began to rapidly increase. Although the lower 0.95 posterior interval is not well constrained, it does appear that this increase occurred less than 50 000 years ago. When we used the slower rate of 0.0075, the initiation of population expansion shifted back to approximately 50 000 years.

As discussed above, the *H. hystrix* data show much lower levels of sequence divergence and population structuring than the *B. scutellaris* data. Because *H. hystrix* is distributed continuously across the beech gap, we dated the age of four relatively well-defined clades in the gene tree and the TMRCA of all haplotypes found within the beech gap. This last method was used to obtain an upper limit on the age of the populations currently in the beech gap. The estimate of TMRCA of all haplotypes sampled from the beech gap populations was between 132 000 years and 588 000 years (Table 4). However, these dates represent an overestimate of the gap closure time because many of these haplotypes are found outside the gap region, suggesting that they diverged from one another well before recolonization of the gap. The height of the tree was between 212 000 to 846 000 years ago. The Bayesian skyline analysis shows that *H. hystrix* underwent a population size expansion somewhere between 60 000 and 20 000 years ago, assuming a rate of 0.0115 and a prior on tree length of 25 (Fig. 8). Using a slower rate of 0.007, the age of the population expansion was 80 000–40 000 years ago.

Nested clade analyses

The 74 haplotypes (113 specimens) of *B. scutellaris* fell into eight unconnected haplotype networks with a maximum of 12 connection steps at the 95% criterion. These included the outgroup, an Auckland group, two groups of East Coast populations, a northwest Nelson/East Coast grouping, a Brady Creek grouping, and two large groups that correspond to A-clade and B-clade in the mtDNA gene tree. We continued with A-clade and B-clade performing nested clade analysis on these two groups separately (Fig. 7A, B).

© 2008 Landcare Research
Journal compilation © 2008 Blackwell Publishing Ltd

Table 4 Dates of time to most recent common ancestor (TMRCA) for *Hisparonia hystrix* data

	Rate = 0.0115 Height = exp(25)	Rate = 0.0115 Height = exp(10)	Rate = 0.007 Height = exp(25)	Rate = 0.007 Height = exp(10)
Node 1	0.278 (0.165–0.393)	0.342 (0.185–0.524)	0.383 (0.230–0.560)	0.513 (0.296–0.772)
Node 2	0.162 (0.075–0.249)	0.185 (0.086–0.294)	0.231 (0.118–0.357)	0.285 (0.146–0.458)
Node 3	0.246 (0.135–0.370)	0.292 (0.147–0.472)	0.337 (0.181–0.501)	0.442 (0.228–0.688)
Node 4	0.301 (0.198–0.422)	0.374 (0.226–0.549)	0.414 (0.249–0.574)	0.559 (0.350–0.810)
Tree height	0.315 (0.212–0.440)	0.4 (0.248–0.592)	0.430 (0.263–0.597)	0.594 (0.362–0.846)
TMRCA beech gap populations	0.237 (0.132–0.351)	0.308 (0.166–0.481)	0.282 (0.157–0.412)	0.388 (0.199–0.588)

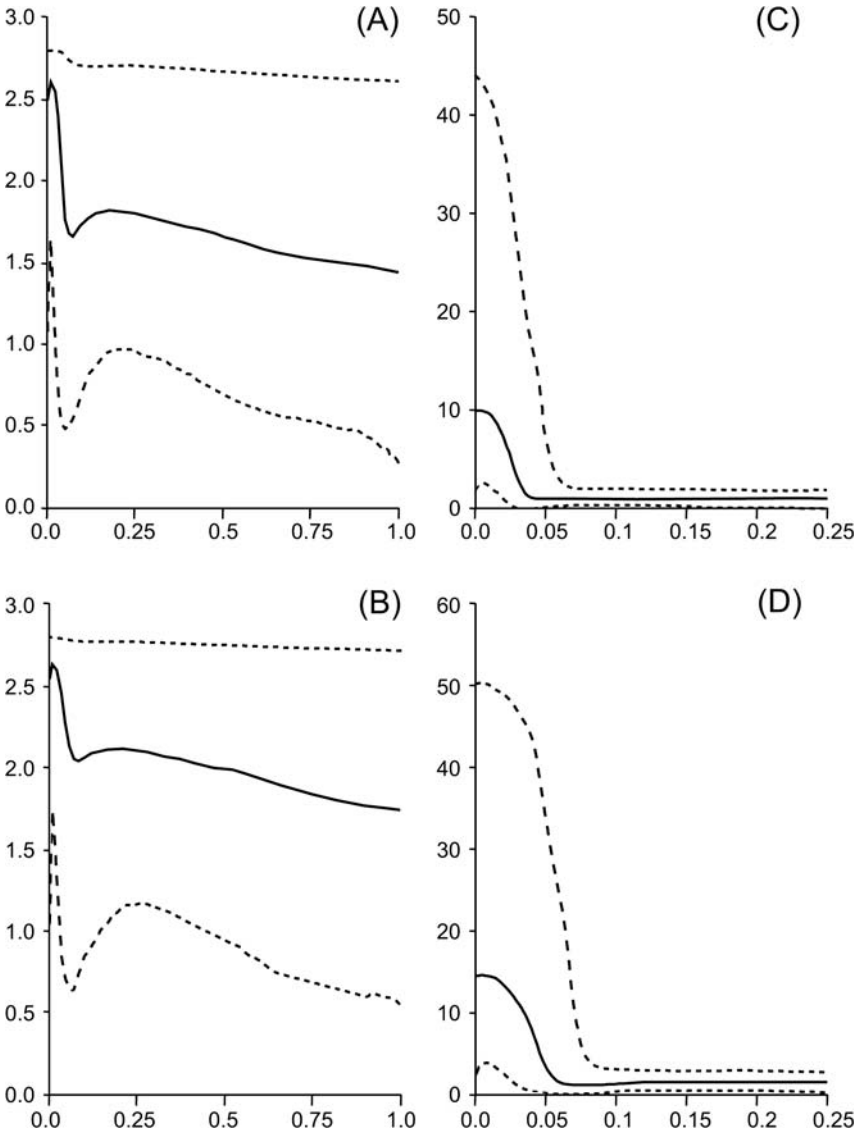

Fig. 6 Bayesian skyline plots showing population size changes through time. The *X*-axis shows time (millions of years) and the *Y*-axis shows relative population size (measured as a product of effective population size and generation time). (A) *Brachynopus scutellaris* (rate = 0.0115); (B) *B. scutellaris* (rate = 0.0075); (C) *Hisparonia hystrix* (rate = 0.0115); and (D) *H. hystrix* (rate = 0.0075).

A-clade. Three ambiguous connections were resolved in the haplotype network following the criteria in Crandall & Templeton (1993), and haplotype 11 was designated as the outgroup. The haplotype network was partitioned into 35 zero-step clades (haplotypes), 22 one-step clades, 12 two-step clades, 6 three-step clades and 3 four-step clades (Fig. 7A). Permutational contingency tests (based on 10 000 resamples) indicated a geographical association of haplotypes in Clades 1-7, 3-4, 4-1, 4-2 and the total cladogram ($P < 0.05$) (Table 5). For the geographical distance analysis, significantly

© 2008 Landcare Research
Journal compilation © 2008 Blackwell Publishing Ltd

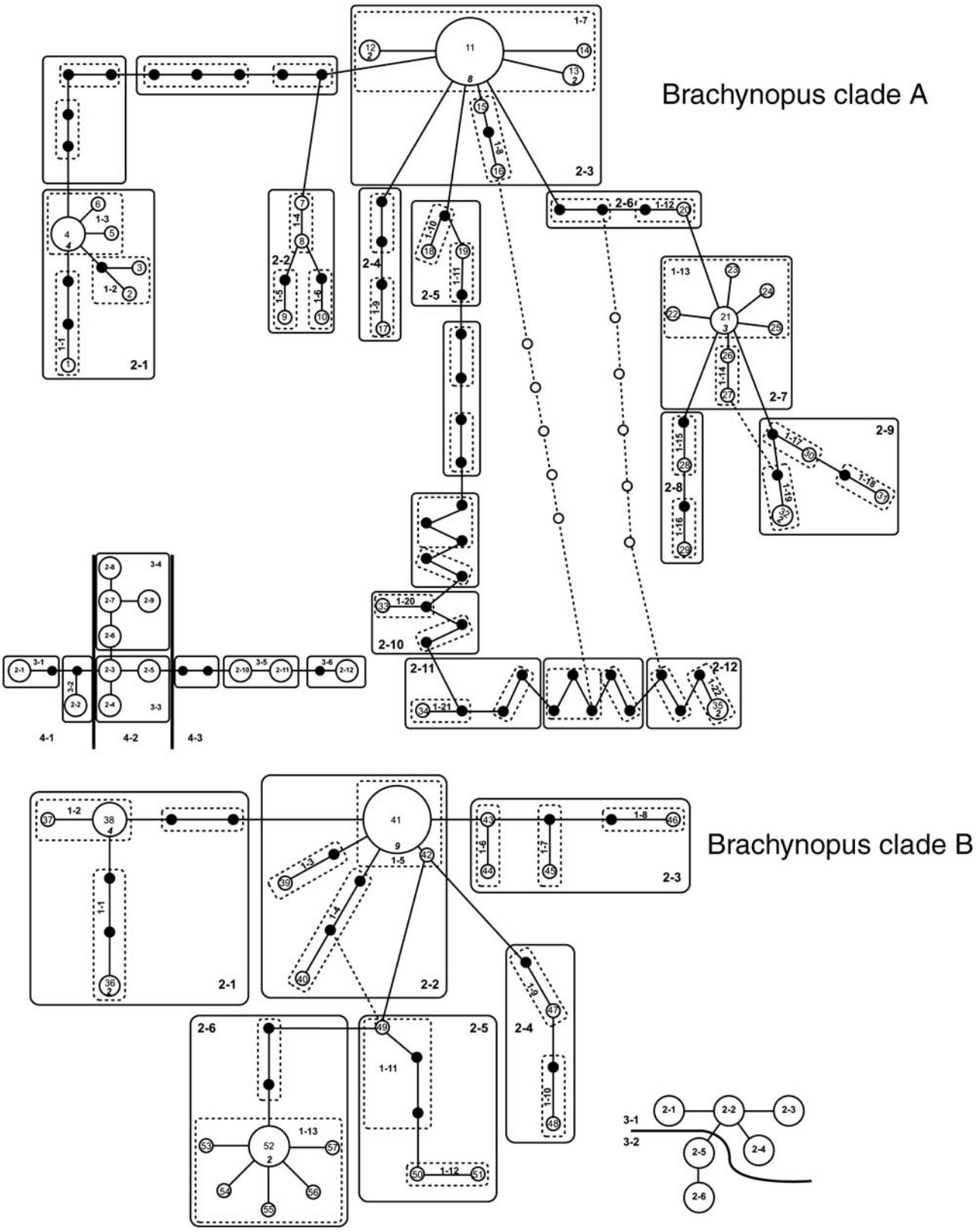

Fig. 7 Nested haplotype network representing relationships within *Brachynopus scutellaris* (A) A-clade, (B) B-clade. Each circle represents a unique haplotype (numbered, Table 5) with size indicating the frequency of that haplotype along with an italicised number for haplotypes with $n > 1$. Solid lines connect haplotypes with a single mutational difference and small solid circles indicate hypothetical historical haplotypes or current haplotypes not sampled. Dashed lines between haplotypes indicate alternative connections. Haplotypes are nested into one-step and two-step clades. Inset A-clade, bottom left, and inset B-clade, bottom right, represent higher level nested design (three-step and four-step clades for A-clade, and 3-step clades for B-clade).

Table 5 Chi-squared test of geographical association and biological inference for clades and from the nested clade analysis of (a) *Brachynopus scutellaris* A-clade (b) *B. scutellaris* B-clade, and (c) *Hisparonia hystrix*. *P* is the probability of obtaining a χ^2 statistic larger than or equal to the observed statistic by randomly permuting the nested contingency results 10 000 times. * indicates clades for which decisions in the inference chain were ambiguous

Clade	χ^2	*P*	Inference chain	Inferred pattern
(a) *B. scutellaris* A-clade				
1-7	20.8542	0.0089	1–2–11–17–No	Inconclusive outcome
3-4*	22.6667	0.0142	1–2_b–$3_{b,c}$–5–No–6	Insufficient genetic resolution to discriminate between range expansion/colonization and restricted dispersal/gene flow
			1–2_b–$3_{b,c}$–5–Yes–15–16–18	Geographical sampling scheme inadequate to discriminate between fragmentation and isolation by distance
4-1	1.0000	0.0210	1–19–20–No	Inadequate geographical sampling
4-2*	34.0000	0.0000	1–19–20–No	Inadequate geographical sampling
			1–19–20–Yes–2–11b–12–No	Contiguous range expansion
Total cladogram	102.0000	0.0000	1–$2_{a,d}$–3–4–No	Restricted gene flow with isolation by distance
(b) *B. scutellaris* B-clade				
2-1	7.0000	0.0485	1–19–20–No	Inadequate geographical sampling
3-1	54.9851	0.0006	1–$2_{a,d}$–3–4–No	Restricted gene flow with isolation by distance
3-2	1.0000	0.0067	1–19–20–2_a–3–4–9–No	Allopatric fragmentation
Total cladogram*	34.4455	0.0000	1–$2_{a,d}$–3–4–No	Restricted gene flow with isolation by distance
			1–$2_{a,d}$–3–4–Yes–9–Yes–10–No	Geographical sampling scheme inadequate to discriminate between fragmentation and isolation by distance
(c) *H. hystrix*				
1-4	48.1875	0.5685	1–$2_{c,d}$–3–4–No	Restricted gene flow with isolation by distance
2-2	44.4444	0.1296	1–$2_{a,d}$–3–4–No	Restricted gene flow with isolation by distance
2-3	9.0000	0.0824	1–19–20–2	Inconclusive outcome (tip/interior status cannot be determined)
2-13	25.4167	0.0119	1–$2_{a,d}$–3–4–No	Restricted gene flow with isolation by distance
3-1	33.5179	0.0050	1–$2_{a,d}$–3–4–No	Restricted gene flow with isolation by distance
3-2	22.5000	0.0080	–	—
3-3*	14.0000	0.0272	1–19–20–No	Inadequate geographical sampling
			1–19–20–Yes–2–11_b–12–No	Contiguous range expansion
3-4*	9.1000	0.0179	1–2_a–3–4–No	Restricted gene flow with isolation
			1–2_a–3–4–Yes–9–No	Allopatric fragmentation
3-5*	1.0000	0.0005	1–19–20–No	Inadequate geographical sampling
			1–19–20–Yes–2–$11_{b,c}$–12–13–14–Yes	Sampling design inadequate to distinguish between contiguous range expansion, long distance colonization and past fragmentation
4-1	137.4360	0.0000	1–2–11_b–12–No	Contiguous range expansion
4-2	31.6667	0.0000	1–2–$11_{b,c}$–12–No	Contiguous range expansion
Total cladogram	88.7758	0.0000	1–$2_{a,c,d}$–3–4–No	Restricted gene flow with isolation by distance

small or large values for D_c, D_n, I-T_c or I-T_n ($P < 0.05$) indicated an association between haplotypes and geography in the same five clades (Table 5). However, although significant genetic–geographical relationships were indicated at the lower nesting levels, inferred patterns were either inconclusive, there was insufficient genetic resolution to discriminate between interpretations of population events or geographical sampling was inadequate. At the four-step level, there is a possibility of contiguous range expansion for Clade 4-2. According to the inference key, restricted gene flow with isolation by distance explains the relationship between clades at the total cladogram level.

B-clade. One ambiguous connection was resolved in the haplotype network, and haplotype 41 was designated as the outgroup. The haplotype network was partitioned into 22 zero-step clades (haplotypes), 13 one-step clades, 6 two-step clades and 2 three-step clades (Fig. 7B). Permutational contingency tests indicated a geographical association of haplotypes mostly at the upper nesting levels, i.e. Clade 2-1, 3-1, 3-2 and the total cladogram ($P < 0.05$) (Table 5). For the geographical distance analysis, significantly small or large values for D_c, D_n, I-T_c or I-T_n ($P < 0.05$) indicated an association between haplotypes and geography in the same four clades (Table 5). For the lowest level, Clade 2-1, no

© 2008 Landcare Research
Journal compilation © 2008 Blackwell Publishing Ltd

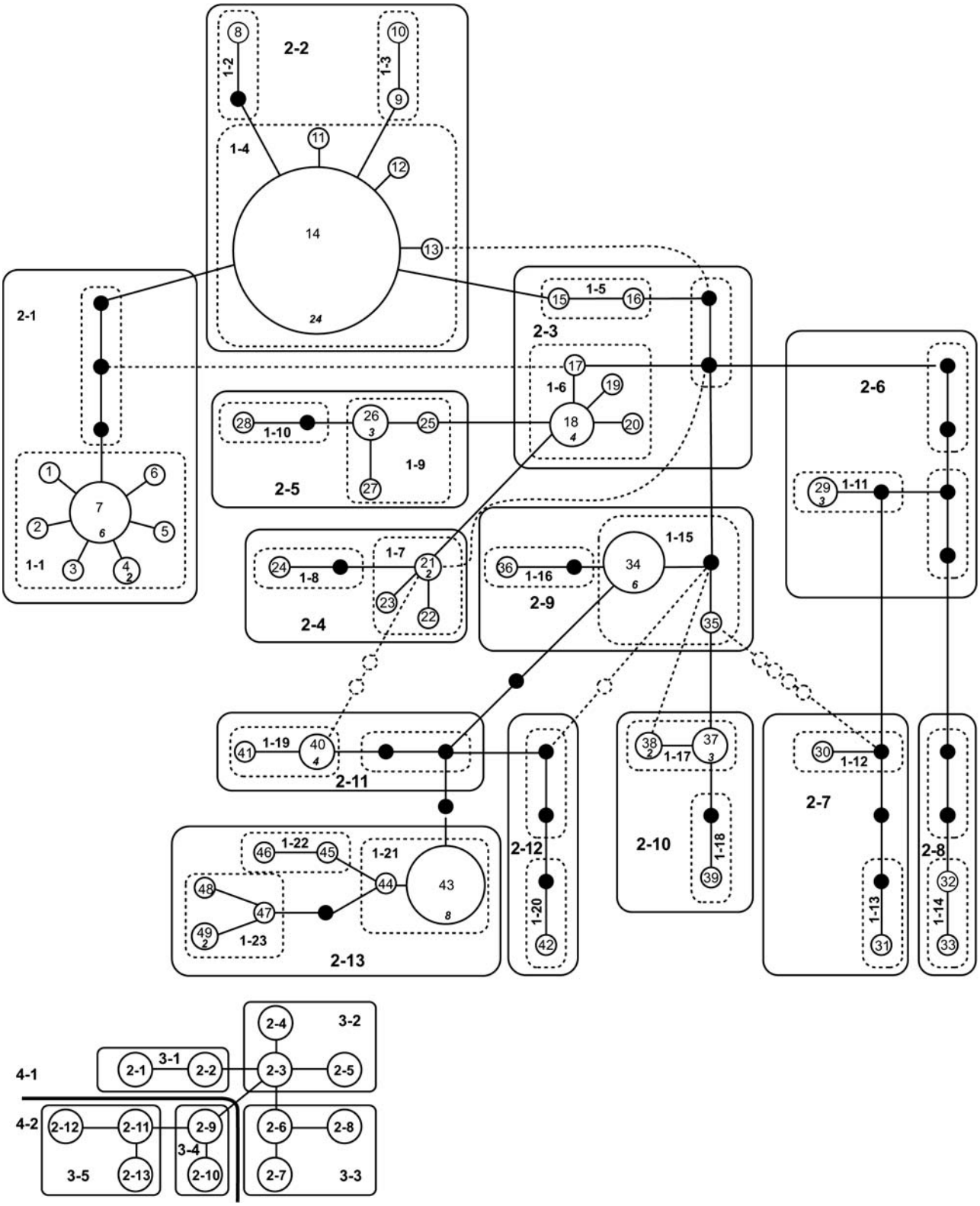

Fig. 8 Nested haplotype network representing relationships within *Hisparonia hystrix*. Each circle represents a unique haplotype (numbered, Table 5) with size indicating the frequency of that haplotype along with an italicised number for haplotypes with $n > 1$. Solid lines connect haplotypes with a single mutational difference and small solid circles indicate hypothetical historical haplotypes or current haplotypes not sampled. Dashed lines between haplotypes indicate alternative connections. Haplotypes are nested into one-step and two-step clades. Inset bottom left: higher level nested design (three-step and four-step clades).

inference could be made due to inadequate sampling. Restricted gene flow with isolation by distance was inferred for Clade 3-1, whereas allopatric fragmentation was inferred for Clade 3-2 which occurs both to the north and to the south of the beech gap. At the total cladogram level, there was not a clear distinction between restricted gene flow with isolation by distance and an inability to distinguish between fragmentation and isolation by distance due to inadequate geographical sampling.

A single haplotype network was constructed using 49 haplotypes (105 specimens) of *H. hystrix*, including two North Island individuals (Waikaremoana and Waipoua), with a maximum of 12 connection steps at the 95% criterion. The biggest outgroup probability was haplotype 14, the most common haplotype with 24 specimens from 15 populations. We resolved 7 ambiguous connections on the haplotype network using the criteria in Crandall & Templeton (1993). Alternative connections between haplotypes are shown as dashed lines in Fig. 8. The haplotype network was partitioned into 49 zero-step clades, 23 one-step clades, 13 two-step clades, 5 three-step clades, and 2 four-step clades (Fig. 8). Permutational contingency tests indicated a geographical association of haplotypes in Clades 2-13, 3-1, 3-2, 3-3, 3-4, 3-5, 4-1, 4-2 and the total cladogram ($P < 0.05$) (Table 5). For the geographical distance analysis, significantly small or large values for D_c, D_n, $I\text{-}T_c$ or $I\text{-}T_n$ ($P < 0.05$) indicated an association between haplotypes and geography in all the above clades, except for Clade 3-2, and in Clades 1-4, 2-2 and 2-3 (Table 5). At the lower nested levels (one- and two-step clades), the inferred pattern was restricted gene flow with isolation by distance, except for Clade 2-3 where the outcome was inconclusive. At the three-step level, inadequate sampling in certain geographical areas prevented clear decisions in the inference process for some clades, although restricted gene flow with isolation was inferred for Clade 3-1. Further sampling in locations identified at this level should allow us to distinguish between short- and long-distance movements to make clearer biological inferences. At the four-step level, contiguous range expansion was inferred for both clades. At the total cladogram level, however, restricted gene flow with isolation by distance explains the relationship between nested clades.

Discussion

Ancient polymorphism and species status in B. scutellaris

Upon cursory examination, it appears that the highly divergent A- and B-clades in *Brachynopus scutellaris* may correspond to separate (cryptic) species. *B. scutellaris* ranges in size from 1.5 to 2.5 mm, and this variation in size is the largest recorded for a single species within the Scaphidiinae (Löbl & Leschen 2003a). In their study, Löbl & Leschen (2003a) dissected over 30 male specimens across the entire geographical range of *B. scutellaris* and found that the internal sac of the genitalia, a key character for species diagnosis, was consistent among all of the specimens. The aedeagus of *B. scutellaris* has a distinctive tripartite anterior sclerite, which it shares with *Brachynopus latus,* and the South American genus *Alexidia* Reitter (Löbl & Leschen 2003b) but it is significantly different in form than the other species that have this structure, making it a reliable morphological feature for species identification.

Typically, specimens of *B. scutellaris* can occur in very high densities and in similar microhabitats (on rotten wood of various tree species) throughout its range. The phylogenetic and biogeographical distribution of haplotypes among the A- and B-clades are similar, though in local subpopulations there is always fixation of one haplotype lineage, with the exception of Pigeon Saddle and Charming Creek. In other cases, populations fixed for different types can be geographically as close as 10 km (e.g. Mount Mclean and Martyr Saddle). The NCA indicated that isolation by distance and restricted gene flow is the dominant pattern in this species, supporting our contention of strong population substructuring. It is likely that the extremely large population size and strong population substructuring in *B. scutellaris* has maintained this polymorphism long-term (e.g. Wakeley 2000). Alternatively, the continual reduction in population size coupled with increased substructuring during ice advances may also cause an increase in coalescent depth (Jesus *et al*. 2006). For these reasons, we believe that *B. scutellaris* is a single species that has maintained two highly divergent haplotype lineages over a long period of time, which we estimate at 896 000–2.9 million years (Table 3).

Biogeographical hypotheses and population divergences dates

Dating recent population divergences. The accuracy of the dates presented here are dependent on a number of assumptions. First, we have assumed that the data are at least approximately clocklike. Although our analyses suggest that rates do indeed vary among lineages, we have used two different substitution rates to partially compensate for this factor. Second, we have assumed that the data are evolving at the rates calculated by Brower (1994) and Quek *et al*. (2004) for arthropod mtDNA. Both of these rate estimates are derived from a number of arthropod studies, and we believe they are likely to be reasonably accurate for the data presented here. We did not apply relaxed clock models (e.g. Thorne & Kishino 2002; but see Drummond *et al*. 2006), because many of these models are based on the assumption that rates of evolution are likely to be inherited and, therefore, autocorrelated across the phylogeny, which may not be the case within species (Kishino *et al*. 2001). Third, the demographic model used in the IM analyses assumed equal population size over time, an assumption

© 2008 Landcare Research
Journal compilation © 2008 Blackwell Publishing Ltd

known to be violated because the Bayes factor and Bayesian skyline analyses clearly favoured an expanding population process. Fourth, we assumed no migration across the beech gap since it formed. This assumption is justified in the case of *B. scutellaris* because we did not observe sharing of haplotypes across the beech gap, and the NCA failed to detect any long-distance dispersal in the data. Finally, because the time estimates from the IM model are scaled by generation time, the estimates of absolute time are dependent on our assumptions regarding generation time. Assuming a shorter generation time will have the effect of decreasing the divergence time and, therefore, shift our estimate for the age of the beech gap closer towards the LGM.

We implemented three methods for dating changes in population demography and distribution. Because these methods are estimating different quantities, comparing them is problematic. The TMRCA method estimates haplotype divergence times, the IM method estimates population divergence times and the Bayesian skyline estimates the time at which population size changes occur. The IM method gives much shallower divergence dates than the TMRCA method due to the well-known discrepancy between population and allelic divergence times (e.g. Edwards & Beerli 2000).

Brachynopus scutellaris. The gene tree topology indicates that the *B. scutellaris* populations to the north and south of the beech gap are genetically distinct and have therefore been isolated for some time. There are no fossils of *B. scutellaris* known from within the beech gap, although there are records from the LGM to the north of the beech gap near Westport (Burge & Shulmeister 2007a, b). The NCA of the B-clade indicates that a vicariant event separated the populations to the north and south of the beech gap. Given that the A- and B-clades are the same species, the lack of support for a vicariant origin for the divergence within the A-clade from the NCA may be the result of limited sample size or topological resolution. Our interpretation of this pattern is that Westland glaciation cleaved the ancestral northern + southern clade into northern and southern populations. The results from the IM analysis suggest that this vicariant event occurred less than 200 000 years ago and so corresponds to Pleistocene glacial cycling. Recent studies of glacial advances in some New Zealand east coast glacial systems have demonstrated that a very substantial glacial advance occurred during the penultimate glaciation (Shulmeister 2005; Rother 2006). This advance was significantly bigger than any in the last ice age and may have eliminated many of the refugia available during other glaciations. The age of this advance (or advances) is still poorly constrained but falls no later than *c*. 150 000 years ago. This older advance may be the event that created the beech gap. However, our date estimates are not precise enough for us to determine whether the vicariant event was the LGM or a more ancient glacial cycle. The southern haplotypes are nested within the radiation of northern haplotypes in both the A- and B-clades. This observation suggests a genetically variable population existed before formation of the beech gap. Since isolation of these two populations, the northern population has yet to obtain reciprocal monophyly despite a long period of isolation. An alternative explanation is that there has been a long-distance dispersal event from the northern populations southwards, across the beech gap. This hypothesis seems less likely and can be rejected because it is not supported by the NCA.

Apart from the beech gap, the overall tree suggests at least three cycles of vicariant events that began in the Late Pliocene or Early Pleistocene (Table 3), inclusive of the north–south split discussed above. The deepest split in the gene tree is between populations from the East Coast of the South Island, the A- and B-clades, and a clade from the North Island and the populations from Brady Creek, east of Haast Pass and Auckland. These divergences are estimated to have occurred earlier in the Pleistocene, and may reflect larger and more ancient advances that occurred earlier in the Pleistocene (Carter 2005). Alternatively, the cause for these earlier divergences may be the increasing effectiveness of the Southern Alps as a biogeographical barrier. Evidence from clast provenance analyses (Mortimer *et al*. 2001) suggest that the Southern Alps propagated northward during the Late Pliocene, reducing west–east biological exchange. Combined with the onset of large-scale glaciation at the end of the Pliocene (see review in Colhoun & Shulmeister 2007), clade divergence at this time is not unexpected (McGlone 1985; Buckley & Simon 2007). The Bayesian skyline analysis shows a large population size increase occurred sometime less than 50 000 years ago, and despite the uncertainty in this date estimate, this is most likely the result of geographical range expansions following the local ice maximum between *c*. 23 000 and 30 000 years ago (Colhoun & Shulmeister 2007). Alternatively, the beetle population explosion may have preceded the last ice maximum because recent studies suggest that climates did not become very extreme at these times (e.g. Marra *et al*. 2006; Woodward & Shulmeister 2007).

Hisparonia hystrix. The biogeographical history of *H. hystrix* differs from *B. scutellaris* and is more complicated to infer from the gene tree topology due to widespread sharing of haplotypes among geographical areas. Furthermore, many of the NCA inferences were inconclusive, but the overall pattern is one of restricted gene flow and isolation by distance. Contiguous range expansion for the two major clades was inferred, and this is consistent with the results from the Bayesian skyline plots, which also show that a major expansion in population size and presumably geographical distribution has occurred between 60 000 and 20 000 years ago.

© 2008 Landcare Research
Journal compilation © 2008 Blackwell Publishing Ltd

The higher levels of genetic diversity in the beech gap region, coupled with a lack of highly divergent unique haplotypes, indicate that this area represents a zone of secondary contact and genetic admixture. The haplotypes sampled from within the beech gap are either shared with or closely related to those found immediately to the north or south of the beech gap, indicating a recent closure of the gap. This pattern may well extend to other taxa, indicating that in addition to being a biotic gap for many taxa, the beech gap is also a more general suture zone (e.g. Remington 1968; Swenson & Howard 2005).

Community assembly and Nothofagus *forest refugia*

The data we have presented here agree with the conclusions of Hall & McGlone (2006) and M. Knapp, K. Stöckler, P. Mardulyn, D. Havell, M. S. McGlone, P. J. Lockhart (in preparation) that recent glacial advances were responsible for the creation of the beech gap. Although we have established that a relatively ancient vicariant event excluded *B. scutellaris* from the beech gap, our genetic data give few clues as to what forces are maintaining its absence. Maintenance of the *B. scutellaris* gap may not be directly related to disturbance as it is in the case of *Nothofagus* for low-altitude regions of Westland (Hall & McGlone 2006). *B. scutellaris* is found on a variety of wood-rotting fungi whose growth is likely to be promoted by forest disturbance and the availability of dead wood. We examined the distribution of the larval hosts of *B. scutellaris* (*Hyphodontia* and other corticioids, Löbl & Leschen 2003a), and these are present and abundant throughout the beech gap (see Anonymous 2007). Moreover, *B. scutellaris* is very abundant, especially in forest edge habitats, and can be collected readily in flight intercept (window) traps (Löbl & Leschen 2003a). It is mysterious that forest disturbance does not promote recolonization of this beetle species into the beech gap. Therefore, we believe that maintenance of the gap in *B. scutellaris* is the result of either an intrinsically slow dispersal rate or simply an absence due to the stochastic nature of community assembly following a disturbance event. This former conclusion is supported by the overall pattern of isolation by distance and restricted gene flow in *B. scutellaris* and perhaps fungal microhabitat associations indicating that populations of *B. scutellaris* are not highly vagile. Local haplotype fixation of either A- or B-clade in all but two localities (Charming Creek and Pigeon Saddle) also supports the hypothesis for slow migration rate between subpopulations.

Disturbance, on the other hand, may have promoted the recolonization of *H. hystrix* into the beech gap. The tea tree *Leptospermum scoparium* is a common early-colonizing species and the recent colonization of *H. hystrix* may have been facilitated in a large part by host use. *H. hystrix* is found on sooty moulds which are abundant on several plant species, such as *L. scoparium* which may occur in primary and secondary forests and scrublands (Carlton & Leschen 2007).

Differential species colonization of the beech gap may be a function of life history. *B. scutellaris* is a forest-floor species, living in a 'two-dimensional' environment, and is sheltered from winds and storms. By contrast, *H. hystrix* is a tree-and-shrub-dwelling species that lives in an environment more exposed to air currents and can be expected to have greater dispersal tendencies than forest-floor dwellers). To further test these hypotheses, more detailed studies on natural history and quantitative genetics are needed (e.g. Bridle & Vines 2006).

Recent biogeographical analysis of New Zealand *Nothofagus* species disjunct across the beech gap (M. Knapp, K. Stöckler, P. Mardulyn, D. Havell, M. S. McGlone, P. J. Lockhart (in preparation)) suggests a pattern of limited gene flow during glacial–interglacial cycles of the Late Pliocene and Pleistocene (~2.4 million–10 000 BP). Our beetle findings differ from the *Nothofagus* results for several methodological reasons, but mainly due to our focus on population genetics within species, and not among species. M. Knapp, K. Stöckler, P. Mardulyn, D. Havell, M. S. McGlone, P. J. Lockhart (in preparation) performed NCA that suggests that fragmentation and range expansion have been the main factors influencing the geographical distribution of *Nothofagus menziesii* chloroplast haplotypes. Fragmentation and range expansion have operated at some level in the fungus beetles, but the overall patterns are either inconclusive or reflect isolation by distance and restricted gene flow. In the case of *B. scutellaris*, isolation by distance and restricted gene flow are consistent with the hypothesis that this is a case of incomplete recolonization into the beech gap. The interplay among genetics, disturbance constraints, and incomplete colonization require additional study, and a fine-grained study of species that have Westland disjunctions is especially warranted.

The beech gap is flanked on the north and south by expansive stands of beech, and the extent of glaciation led McGlone (1985) to suggest that major refugia were likely the source for beech populations that are slowly spreading to Westland. Based on pollen records, Wardle (1980) argued for survival of *Nothofagus* south of the beech gap during recent glacial advances and also raised the possibility of offshore refugia on exposed continental shelf. Leschen & Michaux (2005) also suggested that there could have been an offshore continental shelf refugium during the LGM as an explanation for endemic Westland beetle species, and this could account for the presence of endemic haplotypes in crayfish (Apte *et al*. 2007). The data from *H. hystrix* clearly reveal that source communities are from both the north and the south, and this colonization was followed by extensive admixture in the gap. The geographical distribution and dating of *B. scutellaris* haplotypes also agree with the data

© 2008 Landcare Research
Journal compilation © 2008 Blackwell Publishing Ltd

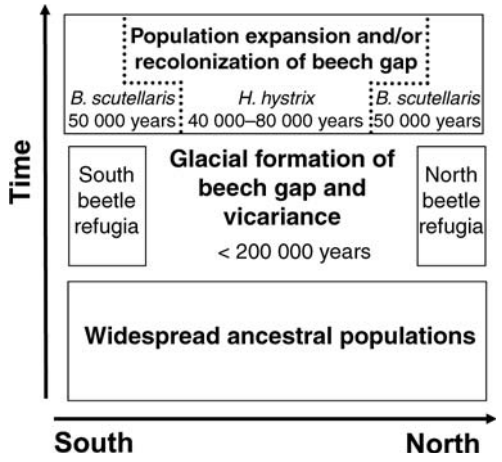

Fig. 9 Summary cartoon representing the Pleistocene history of *Brachynopus scutellaris* and *Hisparonia hystrix*. Dates for the beech gap formation and vicariance are based on IM dating of *B. scutellaris*. Dates for population expansion for both species are based on TMRCA.

for *H. hystrix* that demonstrate that refugia for this species survived in Southern regions of the South Island throughout the LGM.

The biogeographical model we propose for Westland fungus beetles is summarized in Fig. 9. Ancestral widespread beetles that were located throughout the South Island were divided into northern and southern populations by glacial ice advance during 64 000–105 000 years ago (based on IM dating of *B. scutellaris*). These north and south refugia are where *B. scutellaris* is restricted now and are where the source areas for recolonizing populations of *H. hystrix* were present. Population expansion of *B. scutellaris* occurred at 50 000 years ago and recolonization/population expansion of *H. hystrix* occurred 40 000–80 000 years ago based on TMRCM dating.

Acknowledgements

For help in the field or supplying supplemental specimens, we thank Grace Hall, Robert Hoare, Tony Jewell, Paul Lambert, Dave Seldon, Darren Ward and the Lake Waikaremoana Restoration Trust. Baxter Massey and Robyn Howitt assisted in the laboratory and Alexei Drummond provided critical advice on methods of analysis. Fraser Morgan helped with generating the distribution maps, Des Helmore drew the habitus of *B. scutellaris*, and Birgit Rhode photographed *H. hystrix*. Dianne Gleeson, Trevor Crosby, and David Choquenot provided additional support. For reviews of this paper, we thank Chris Burridge, Brent Emerson, Hannah Buckley, David Marshall, Katie Marske, and Matt McGlone. Funding for this project was provided by the Foundation for Research, Science and Technology (contract CO9/0501) and Royal Society of New Zealand Marsden grants UOC301 (J. Shulmeister and R. Leschen, principal investigators) and LCR0502 (T.R. Buckley, principal investigator).

© 2008 Landcare Research
Journal compilation © 2008 Blackwell Publishing Ltd

References

Anonymous [Herbarium PDD] (2007) NZFUNGI Database of New Zealand Fungi. Landcare Research, New Zealand. http://nzfungi.landcareresearch.co.nz/.

Akaike H (1973) Information theory and an extension of the maximum likelihood principle. In: *Second International Symposium on Information Theory*, pp. 267–281. Akademiai Kiado, Budapest.

Apte S, Smith PJ, Wallis GP (2007) Mitochondrial phylogeography of New Zealand freshwater crayfishes, *Paranephrops* spp. *Molecular Ecology*, **16**, 1897–1908.

Bridle JR, Vines TH (2006) Limits to evolution at range margins: when and why does adaptation fail? *Trends in Ecology & Evolution*, **22**, 140–147.

Brower AVZ (1994) Rapid morphological radiation and convergence in geographical races of the butterfly, *Heliconius erato*, inferred from patterns of mitochondrial DNA evolution. *Proceedings of the National Academy of Sciences*, **91**, 6491–6495.

Buckley TR, Simon C (2007) Evolutionary radiation of the cicada genus *Maoricicada* Dugdale (Hemiptera: Cicadoidea) and the origins of the New Zealand alpine biota. *Biological Journal of the Linnaean Society*, **91**, 419–435.

Buckley TR, Simon C, Chambers GK (2001a) Phylogeography of the New Zealand cicada *Maoricicada campbelli* based on mitochondrial DNA sequences: ancient clades associated with Cenozoic environmental change. *Evolution*, **55**, 1395–1407.

Buckley TR, Simon C, Chambers GK (2001b) Exploring among-site rate variation models in a maximum likelihood framework using empirical data: effects of model assumptions on estimates of topology, branch lengths and bootstrap support. *Systematic Biology*, **50**, 67–86.

Burge PI, Shulmeister J (2007a) An OIS 5a to OIS 4 (or early OIS 3) environmental and climatic reconstruction from the northwest, South Island, New Zealand, using beetle fossils. *Journal of Quaternary Science*, **22**, 501–516.

Burge PI, Shulmeister J (2007b) Re-envisioning the structure of New Zealand vegetation during the last glaciation using beetle fossils. *Quaternary Research*, **68**, 121–132.

Burrows JC (1965) Some discontinuous distributions of plants within New Zealand and their ecological significance. II. Disjunctions between Otago-Southland and Nelson Marlborough and related distribution patterns. *Tuatara*, **13**, 9–29.

Carlton CE, Leschen RAB (2007) Descriptions of *Soronia* complex (Nitidulidae: Nitiduline) larvae of New Zealand with comments on life history and taxonomy. *New Zealand Entomologist*, **30**, 41–51.

Carter RM (2005) A New Zealand climatic template back to *c*. 3.9 Ma: ODP Site 1119, Canterbury Bight, south-west Pacific Ocean, and its relationship to onland successions. *Journal of the Royal Society of New Zealand*, **35**, 9–42.

Clement M, Posada D, Crandall KA (2000) TCS: a computer program to estimate gene genealogies. *Molecular Ecology*, **9**, 1657–1660.

Cockayne L (1926) Monograph on the New Zealand beech forests. Part I. The ecology of the forests and taxonomy of the beeches. *Bulletin of the New Zealand State Forest Service* **4**, Wellington.

Cockayne L (1928) *The Vegetation of New Zealand*, 2nd edn. Engelmann Press, Leipzig.

Colhoun E, Shulmeister J (2007) Glaciation of the South West Pacific. In: *Encyclopaedia of Quaternary Science* (ed. Elias S), pp. 1066–1075. Elsevier, London.

Crandall KA, Templeton AR (1993) Empirical tests of some predictions from coalescent theory with applications to intraspecific phylogeny reconstruction. *Genetics*, **134**, 959–969.

Drummond AJ, Rambaut A (2006) BEAST version 1.4, Available from http://beast.bio.ed.ac.uk/.

Drummond AJ, Nicholls GK, Rodrigo AG, Solomon W (2002) Estimating mutation parameters, population history and genealogy simultaneously from temporally spaced sequence data. *Genetics*, **161**, 1307–1320.

Drummond AJ, Rambaut A, Shapiro B, Pybus OG (2005) Bayesian coalescent inference of past population dynamics from molecular sequences. *Molecular Biology and Evolution*, **22**, 1185–1192.

Drummond AJ, Ho SYW, Philips MJ, Rambaut A (2006) Relaxed phylogenetics and dating with confidence. *Public Library of Science, Biology*, **4**, e88.

Edwards SV, Beerli B (2000) Perspective: gene divergence, population divergence, and the variation in coalescence time in phylogeographic studies. *Evolution*, **54**, 1839–1854.

Gu X, Fu YX, Li WH (1995) Maximum likelihood estimation of the heterogeneity of substitution rate among nucleotide sites. *Molecular Biology and Evolution*, **12**, 546–557.

Haase P (1990) Environmental and floristic gradients in Westland, New Zealand, and the discontinuous distribution of *Nothofagus*. *New Zealand Journal of Botany*, **28**, 25–40.

Hall GMJ, McGlone MS (2006) Potential forest cover of New Zealand as determined by an ecosystem process model. *New Zealand Journal of Botany*, **44**, 211–232.

Hasegawa M, Kishino H, Yano T (1985) Dating the human-ape split by a molecular clock of mitochondrial DNA. *Journal of Molecular Evolution*, **22**, 160–174.

Huelsenbeck JP, Imennov NS (2002) Geographic origin of human mitochondrial DNA: accommodating phylogenetic uncertainty and model comparison. *Systematic Biology*, **51**, 155–165.

Hughes SJ (1976) Sooty moulds. *Mycologia*, **68**, 693–820.

Jesus FF, Wilkins JF, Solferini VN, Wakeley J (2006) Expected coalescent times and segregating sites in a model of glacial cycles. *Genetics and Molecular Research*, **5**, 466–474.

Jukes TH, Cantor CR (1969) Evolution of protein molecules. In: *Mammalian Protein Metabolism* (ed. Munro NH), pp. 21–123. Academic Press, New York.

Kass RE, Raftery AE (1995) Bayes factors. *Journal of the American Statistical Association*, **90**, 773–795.

Kirejtshuk AG (2003) Four new genera of the *Soronia* complex (Coleoptera: Nitidulidae) from Australia, New Zealand, Fiji and tropical America with notes on composition of the complex and description of new species from Southern Hemisphere. *Russian Entomological Journal*, **12**, 239–256.

Kishino H, Thorne JL, Bruno WJ (2001) Performance of a divergence time estimation method under a probabilistic model of rate evolution. *Molecular Biology and Evolution*, **18**, 352–361.

Kuhner MK, Yamato J, Felsestein J (1998) Maximum likelihood estimation of population growth rates based on coalescent. *Genetics*, **149**, 429–434.

Lanave C, Preparata G, Saccone C, Serio G (1984) A new method for calculating evolutionary substitution rates. *Journal of Molecular Evolution*, **20**, 86–93.

Leathwick JR (1998) Are New Zealand's *Nothofagus* species in equilibrium with their environment? *Journal of Vegetation Science*, **9**, 719–732.

Leathwick JR, Morgan F, Wilson G, Rutledge D, McLeod M, Johnston K (2003) *Land Environments of New Zealand Technical Guide*. David Bateman, Auckland.

Leschen RAB, Löbl I (2005) Phylogeny and classification of Scaphisomatini (Staphylinidae: Scaphidiinae) with notes on mycophagy, termitophily, and functional morphology. *Coleopterists Society Monographs*, **3**, 1–63.

Leschen RAB, Michaux B (2005) Phylogeny and evolution of New Zealand Priasilphidae (Coleoptera). *New Zealand Journal of Entomology*, **28**, 55–64.

Löbl I, Leschen RAB (2003a) *Scaphidiinae (Insecta: Coleoptera: Staphylinidae). Fauna of New Zealand Number 48*. Manaaki Whenua Press, Lincoln, New Zealand.

Löbl I, Leschen RAB (2003b) Redescription and new species of *Alexidia* (Staphylinidae: Scaphidiinae). *Revue Suisse de Zoologie*, **110**, 315–324.

Marra MJ, Shulmeister J, Smith ECG (2006) Reconstructing temperature during the Last Glacial Maximum from Lyndon Stream, South Island, New Zealand using beetle fossils and maximum likelihood envelopes. *Quaternary Science Reviews*, **25**, 1841–1849.

McDowall RM (1997) Indigenous vegetation type and the distribution of short-jawed kokopu, *Galaxia postvectic* (Teleosti: Galaxiidae), in New Zealand. *New Zealand Journal of Zoology*, **24**, 243–255.

McDowall RM (2005) Historical biogeography of the New Zealand freshwater crayfishes (Parastacidae, *Paranephrops* spp.): restoration of a refugial survivor? *New Zealand Journal of Zoology*, **32**, 55–77.

McGlone MS (1985) Plant biogeography and the late Cenozoic history of New Zealand. *New Zealand Journal of Botany*, **23**, 723–749.

McGlone MS, Mildenhall DC, Pole MS (1996) The history and paleoecology of New Zealand *Nothofagus* forests. In: *Nothofagus: Ecology and Evolution* (eds Veblen TT Hill RS Read J), pp. 83–130. Yale University Press, New Haven, Connecticut.

Mortimer N, Sutherland R, Nathan S (2001) Torlesse greywacke and Haast Schist source for Pliocene conglomerates near Reefton, New Zealand. *New Zealand Journal of Geology and Geophysics*, **44**, 105–111.

Neilsen R, Wakeley J (2001) Distinguishing migration from isolation: a Markov chain Monte Carlo approach. *Genetics*, **158**, 885–896.

Newton MA, Raftery AE (1994) Approximate Bayesian inference with the weighted likelihood bootstrap (with discussion). *Journal of the Royal Statistical Society (Series B)*, **56**, 3–48.

Nylander JAA, Ronquist F, Huelsenbeck JP, Nievea-Aldrey JL (2004) Bayesian phylogenetic analysis of combined data. *Systematic Biology*, **53**, 47–67.

Posada D, Buckley TR (2004) Model selection and model averaging in phylogenetics: advantages of the AIC and Bayesian approaches over likelihood ratio tests. *Systematic Biology*, **53**, 793–808.

Posada D, Crandall KA (1998) MODELTEST: testing the model of DNA substitution. *Bioinformatics*, **14**, 817–818.

Posada D, Crandall KA, Templeton AR (2000) GEODIS: a program for the cladistic nested analysis of the geographical distribution of genetic haplotypes. *Molecular Ecology*, **9**, 487–488.

Pybus OG, Rambaut A, Harvey PH (2000) An integrated framework for the inference of viral population history from reconstructed genealogies. *Genetics*, **155**, 1429–1437.

Quek S-P, Davies SJ, Itino T, Pierce NE (2004) Codiversification in an ant–plant mutualism: stem texture and the evolution of host use in *Crematogaster* (Formicidae: Myrmicinae) inhabitants of *Macaranga* (Euphorbiaceae). *Evolution*, **58**, 554–570.

Remington CL (1968) Suture–zones of hybrid interaction between recently joined biotas. In: *Evolutionary Biology* (eds Dobzhansky T, Hetch MK, Steere WC), pp. 321–428. Plenum, New York.

© 2008 Landcare Research
Journal compilation © 2008 Blackwell Publishing Ltd

Rother H (2006) *Late Pleistocene glacial geology of the Waiau-Hope Valley system in North Canterbury, New Zealand*. Unpublished PhD Thesis, University of Canterbury, Christchurch, New Zealand.

Rozas J, Sánchez-DelBarrio JC, Messeguer X, Rozas R (2003) DNASP, DNA polymorphism analyses by the coalescent and other methods. *Bioinformatics*, **19**, 2496–2497.

Shulmeister J (2005) The nature and timing of mountain glaciation in Australasia between *c.* 130 and 10 ka. *Geological Society of America Annual Meeting*, 15–19 October 2005, Salt Lake City, Utah.

Simon C, Frati F, Crespi B, Liu H, Flook PK (1994) Evolution, weighting, and phylogenetic utility of mitochondrial gene sequences and a compilation of conserved PCR primers. *Annals of the Entomological Society of America*, **87**, 651–701.

Suggate RP (1990) Late Pliocene and Quaternary glaciations of New Zealand. *Quaternary Science Reviews*, **9**, 175–197.

Suggate RP, Almond PC (2005) The Last Glacial Maximum (LGM) in western South Island, New Zealand: implications for the global LGM and MIS 2. *Quaternary Science Reviews*, **24**, 1923–1940.

Swenson NG, Howard DJ (2005) Clustering of contact zones, hybrid zones, and phylogeographic breaks in North America. *American Naturalist*, **166**, 581–591.

Swofford DL (1998) PAUP*. *Phylogenetic Analysis Using Parsimony (*and Other Methods)*, Version 4. Sinauer Associates, Sunderland, Massachusetts.

Tajima (1989) Statistical method for testing the neutral mutation hypothesis by DNA polymorphism. *Genetics*, **123**, 585–595.

Templeton AR (1998) Nested clade analyses of phylogeographic data: testing hypotheses about gene flow and population history. *Molecular Ecology*, **7**, 381–397.

Templeton AR, Sing CF (1993) A cladistic analysis of phenotypic associations with haplotypes inferred from restriction endonuclease mapping. IV. Nested analyses with cladogram uncertainty and recombination. *Genetics*, **134**, 659–669.

Templeton AR, Boerwinkle E, Sing CF (1987) A cladistic analysis of phenotypic associations with haplotypes inferred from restriction endonuclease mapping. I. Basic theory and an analysis of alcohol dehydrogenase activity in *Drosophila*. *Genetics*, **117**, 343–351.

Templeton AR, Crandall KA, Sing CF (1992) A cladistic analysis of phenotypic associations with haplotypes inferred from restriction endonuclease mapping and DNA sequence data. III. Cladogram estimation. *Genetics*, **132**, 619–633.

Templeton AR, Routman E, Phillips CA (1995) Separating population structure from population history: a cladistic analysis of the geographical distribution of mitochondrial DNA haplotypes in the tiger salamander, *Ambystoma tigrinum*. *Genetics*, **140**, 767–782.

Thompson JD, Higgins DG, Gibson TJ (1994) CLUSTAL W: improving the sensitivity of progressive multiple sequence alignment through sequence weighting, position specific gap penalties and weight matrix choice. *Nucleic Acids Research*, **22**, 4673–4680.

Thorne JL, Kishino H (2002) Divergence time and evolutionary rate estimation with multilocus data. *Systematic Biology*, **51**, 689–702.

Wakeley J (2000) The effects of subdivision on the genetic divergence of populations and species. *Evolution*, **54**, 1092–1101.

Wardle P (1963) Evolution and distribution of the New Zealand flora, as affected by Quaternary climates. *New Zealand Journal of Botany*, **1**, 3–17.

Wardle P (1964) Facets of the distribution of the forest vegetation in New Zealand. *New Zealand Journal of Botany*, **2**, 352–366.

Wardle P (1980) Ecology and distribution of silver beech (*Nothofagus menziesii*) in the Paringa district, South Westland, New Zealand. *New Zealand Journal of Ecology*, **3**, 23–34.

Wardle P, Harris W, Buxton RP (1988) Effects of glacial climates on floristic distributions in New Zealand. 2. The role of long-distance hybridization in disjunct distributions. *New Zealand Journal of Botany*, **26**, 557–564.

Woodward CA, Shulmeister J (2007) Chironomid-based reconstructions of air temperature and phytoplankton productivity (chlorophyll *a*) from lake deposits in Lyndon Stream, New Zealand. Implications for environmental conditions during the New Zealand Last Glacial Maximum (LGM). *Quaternary Science Reviews*, **27**, 142–154.

Yang Z (1994) Estimating the pattern of nucleotide substitution. *Journal of Molecular Evolution*, **39**, 105–111.

Yang Z, Rannala B (2005) Branch-length prior influences Bayesian posterior probability of phylogeny. *Systematic Biology*, **54**, 455–470.

Richard Leschen is a coleopterist specializing on the systematics and evolution of fungus-feeding microcoleoptera worldwide. He has been collaborating on work with geologists, biogeographers, and geneticists to determine the biological and geological history of New Zealand. Thomas Buckley studies the systematics, biogeography and population genetics of New Zealand terrestrial invertebrates, with a special focus on stick insects. Helen Harman is a research scientist whose interests includes population genetics and ecology of invasive species and introduced biocontrol agents. Jamie Shulmeister is a paleoclimatologist and his research is focused on the causes of ice ages and on the geological history of the Southern Hemisphere westerlies. He has cross-over interests in paleoecology and has been responsible for developing several micro-fauna and flora groups for use in paleoecological and paleoclimatic work.

© 2008 Landcare Research
Journal compilation © 2008 Blackwell Publishing Ltd